Applied Catalysis B: Environmental 152–153 (2014) 218–225

Contents lists available at ScienceDirect

Applied Catalysis B: Environmental

journal homepage: www.elsevier.com/locate/apcatb

Improved low-temperature activity of silver–alumina for lean NO_x reduction – Effects of Ag loading and low-level Pt doping

Fredrik Gunnarsson*, Hannes Kannisto, Magnus Skoglundh, Hanna Härelind

Competence Centre for Catalysis, Department of Chemical and Biological Engineering, Chalmers University of Technology, SE-412 96 Göteborg, Sweden

ARTICLE INFO

Article history:
Received 31 October 2013
Received in revised form
27 December 2013
Accepted 15 January 2014
Available online 31 January 2014

Keywords:
Silver–alumina
Ag/Al_2O_3
HC-SCR
Platinum doping
Lean NO_x reduction

ABSTRACT

This study focuses on the effect of silver loading and low-level platinum doping on the distribution of silver species, the hydrocarbon activation, and the low-temperature activity for lean NO_x reduction over silver–alumina catalysts. Sol–gel prepared Ag/Al_2O_3 samples, with varying silver loading and doped with trace amounts of platinum, were evaluated as HC-SCR catalysts using *n*-octane as reductant in a synthetic gas-bench reactor. In addition, the samples were characterized using X-ray photoelectron spectroscopy, ultraviolet visible spectroscopy, and the specific surface area was determined using nitrogen sorption. The study shows that as the samples are doped with trace-amounts of platinum, the activity for lean NO_x reduction at low temperatures is enhanced. The catalyst composition that displays the highest activity for NO_x reduction is a 2 wt% Ag/Al_2O_3 sample doped with 500 ppm platinum. This catalyst displays the highest low-temperature activity, most likely owing to an increased ability to adsorb and partially oxidize the hydrocarbon reductant, which is attributed to the Pt doping. Adsorption of a higher amount of hydrocarbons could result in that a lower amount of reducing agent is required for Pt doped Ag–alumina catalysts as compared to un-doped ones, which is beneficial with respect to fuel efficiency.

1. Introduction

Stringent emission legislations and limited fossil fuel resources are strong drivers for energy-efficient engine concepts, such as diesel and lean-burn engines [1]. These engines use higher oxygen concentrations in the combustion chamber, i.e. higher air-to-fuel (A/F) ratios, which results in a more complete combustion, decreasing the fuel consumption and thus the emissions of anthropogenic CO_2, compared to engine concepts based on stoichiometric combustion. The emission restrictions of today consider particulate matter (PM) and nitrogen oxides (NO_x). Emissions of NO_x are hazardous to the environment, acting as a source to ground level ozone, acid rain and eutrophication, as well as being directly harmful to humans [2,3]. The legislated maximum emission levels of NO_x for heavy-duty vehicles have been reduced from 8.0 g/kWh in 1992 (Euro I), to 0.4 g/kWh in the Euro VI levels, which are to be implemented in 2013 [1]. Solving the problem of NO_x emission abatement is therefore of crucial importance. The conventional technique to reduce NO_x emissions has been the three-way-catalyst (TWC). However, the lean environment in the exhaust gas from diesel and lean-burn engine systems obstructs the NO_x reduction in the TWC, as these systems operate at high A/F ratios [4]. One possible technique circumventing this problem, is selective catalytic reduction of NO_x using either hydrocarbons, i.e. fuel or derivates from the fuel, (HC-SCR), or urea which decomposes to ammonia (NH_3-SCR), as the reducing agent [5]. Although urea is readily available in many countries, e.g. USA and most parts of Europe, access to urea is still very limited in the larger part of the world. An advantage with the HC-SCR system is that as the fuel is used as reducing agent, no additional component is needed and the system can be utilized for automotives world-wide. Silver–alumina (Ag/Al_2O_3) has been pointed out as a potential catalyst for HC-SCR, displaying promising results for a variety of hydrocarbons, including fossil fuels and bio-fuels [6,7]. One drawback with the Ag/Al_2O_3 system has been that the system requires relatively high temperatures to achieve high activity, whereas the energy-efficiency in engines increases, the exhaust gas temperature decreases. Many new engine designs also include heat recovery systems, which decrease the temperature of the exhaust gas reaching the catalyst even further. Nevertheless, the active temperature window for HC-SCR over Ag/Al_2O_3 may be shifted towards lower temperatures, provided a small amount of hydrogen is introduced to the exhaust gas feed [8]. The addition of hydrogen further results in an over-all increase in the NO_x reduction, where the highest activity generally has been reported over Ag/Al_2O_3 catalysts containing 2 wt% Ag [9,10]. The added hydrogen does however increase the fuel-penalty, as it is produced from on-board fuel-reforming. Recently Kannisto et al. [11] have shown that hydrogen levels as low as 1000 ppm result in a fuel penalty of about 2%, cf. 0.5% for urea-SCR.

* Corresponding author. Tel.: +46 (0) 31 772 33 72.
E-mail address: fredrik.gunnarsson@chalmers.se (F. Gunnarsson).

0926-3373/$ – see front matter © 2014 Elsevier B.V. All rights reserved.
http://dx.doi.org/10.1016/j.apcatb.2014.01.043

The main reactions in HC-SCR are the NO_x reduction, facilitated by the hydrocarbon reductant, and the competing combustion reaction, where the hydrocarbon is oxidized by oxygen. To favor the desired reaction and to achieve high performance at low temperatures, the hydrocarbon needs to be activated, i.e. partially oxidized, before reacting with the NO_x to form N_2 [12,13]. Although the complete reaction mechanism is still under debate, several active sites are likely involved e.g. silver ions, small silver clusters and larger metallic silver particles [14–16]. The oxidation potential of the oxidation sites is of crucial importance, as the hydrocarbon needs to be partially oxidized but prevented from being combusted. Strategies to facilitate the partial oxidation of the hydrocarbon may be to incorporate additional oxidation sites in the Ag–alumina catalyst or by altering the oxidizing potential of the existing oxidation sites. Previous studies [11] indicate that trace amounts of platinum incorporated in the silver–alumina catalyst can increase the maximum NO_x conversion and, at the same time, decrease the onset temperature of the HC-SCR reaction. It has also been proposed by Liu et al. [17] that the addition of platinum, via $PtCl_2$ and CO sublimation, enhances the adsorption of hydrocarbons which was found to facilitate the NO_x reduction at low temperatures since more hydrocarbons are available on the surface. The authors ascribe the increase in HC adsorption to a change in the acidity of the surface, owing to chlorine residues from the synthesis [17]. Furthermore, Sato et al. have observed a decrease in activity when adding Pt, while the addition of Rh results in an improvement of the activity [18]. However, the experimental conditions in the present study differ substantially compared to the conditions in the paper from Sato et al.

The objective of this study is to increase the understanding of the effects of silver loading and the role of platinum doping on the distribution of silver species, the hydrocarbon activation, and the catalytic activity for lean NO_x reduction over silver–alumina catalysts, with special focus on the low-temperature regime relevant for diesel- and lean-burn applications.

2. Experimental methods

2.1. Sample preparation

Ag/Al_2O_3 samples were prepared by a sol–gel based method including freeze-drying, which has shown improved properties cf. impregnated samples [14], with a nominal silver loading of 2 and 6 wt%, respectively. In addition, the corresponding samples were prepared with addition of 100 and 500 ppm platinum, respectively. The catalysts are denoted as: Ag (silver loading in %) Pt (platinum doping in ppm), i.e. the sample containing 2 wt% Ag and 500 ppm Pt is denoted Ag2Pt500. The alumina precursor (aluminum isopropoxide, >98%, Aldrich) was added to milli-Q water and heated to 82 °C during vigorous stirring. Subsequently, the silver precursor ($AgNO_3$, >99%, Sigma), and for the Pt doped samples a platinum precursor ($Pt(NO_3)_2$, solution type K, Heraeus), were added. The pH was adjusted to 4.5 by addition of HNO_3 (10%, Fluka), resulting in the formation of a sol. The sol was stirred for 12 h, after which a major part of the solvent was removed using a heated vacuum system. The resulting gel was freeze-dried in order to preserve the microporous structure of the aluminum oxy-hydroxide and to minimize the migration of silver in the pores during the drying process. The resulting cryogels were calcined in air at 600 °C for 6 h and finally ground to a fine powder. The powder was then wash-coated onto cordierite monoliths (Corning, 400 cpsi, OD/L = 20/20 mm) as described in Ref. [14]. A wash-coat slurry with 20 wt% dry content was prepared, where the dry part consisted of 20 wt% AlOOH-binder (Disperal P2, Condea) and 80 wt% catalyst powder. The monolith were submerged in the slurry, dried at 90 °C for 15 min and then subjected to a fast calcination at 600 °C in air for 2 min. The procedure was repeated until the desired amount of wash-coat was acquired, where after the coated monolith samples were calcined in air (600 °C, 3 h).

2.2. Sample characterization

The specific surface area of the powder samples was determined by nitrogen sorption (Micrometrics Tristar 3000) at 77 K and applying the BET method [19]. The samples were dried in vacuum at 225 °C for 2 h before the measurements.

The type and relative amount of silver species in the powder samples were investigated using ultraviolet-visible (UV–Vis) diffuse reflectance spectroscopy. Here, a γ-alumina sample, prepared using the same procedure as the silver–alumina samples, was used as reference. The samples were investigated in the range between 200 and 1500 nm using a Cary 5000 spectrometer, with a Labsphere Spectralon as reference.

The silver species were further investigated using X-ray photoelectron spectroscopy (XPS). The powder samples were pressed to approximately 0.5 mm thick wafers and studied using a PerkinElmer PHI 5000C instrument, with a monochromatic Al K_α source. Charging of the samples was accounted for by calibrating the spectra using the C1s peak at 284.5 eV as reference [20].

2.3. Flow-reactor experiments

2.3.1. Activity measurements

The catalytic performance of the monolith samples for lean NO_x reduction was evaluated at steady-state conditions in a continuous gas flow reactor, described in detail previously by Kannisto et al. [14]. The flow-reactor consisted of a horizontally mounted quarts tube (ID/L = 22/800 mm), which was heated by a metal coil and insulated with quartz-wool. The monolith sample was placed close to the outlet, maximizing the gas heating, with uncoated monoliths before and after the sample to minimize heat-losses from radiation. The temperature was measured using type K thermocouples and controlled by PID-controllers (Eurotherm). The inlet gas composition (200 ppm NO, 1000 ppm H_2, 10% O_2 and Ar_{bal}) was controlled by separate mass flow controllers (Bronkhorst Hi-tech) and the outlet gas composition was analyzed using a FTIR gas-analyzer (MKS 2030 HS). Water (corresponding to 5%) and hydrocarbon were introduced separately to the reactor chamber via controlled evaporator mixer systems (CEM, Bronkhorst Hi-Tech). The total gas flow was 3,500 mL/min, resulting in GHSV = 33,200 h^{-1}.

The catalyst samples were initially conditioned in 10% oxygen and argon at 550 °C, after which they were investigated at steady-state conditions for 30 min between 400 and 225 °C in 25 °C steps, using *n*-octane as reducing agent. The C/N molar ratio was kept constant at 6 during all experiments, corresponding to a C_1-concentration of 1200 ppm. Total oxidation of the hydrocarbon over a commercial TWC catalyst at 500 °C, resulted in a C_1 concentration of 1150 ppm, which may be considered within the experimental errors. Formation of nitrogen containing species, other than NO and NO_2, i.e. NH_3, HNCO, N_2O and cyanide species, were monitored and the concentrations were determined to be negligible (well below 5 ppm). Hence these species were excluded from the NO_x reduction calculations, which were derived in accordance with Eqs. (1) and (2).

$$NO_x = NO + NO_2 \quad (1)$$

$$NO_x\text{reduction}(\%) = 100 * (NO_{x,in} - NO_{x,out})/NO_{x,in} \quad (2)$$

The hydrocarbon conversion was determined according to Eqs. (3) and (4).

$$C_{1,out} = CO_{out} + CO_{2,out} \quad (3)$$

$$HCconversion(\%) = 100 * (C_{1,out}/C_{1,in}) \quad (4)$$

2.3.2. Hydrocarbon and NO oxidation

One key-property of the Ag/Al_2O_3 catalyst is, as stated above, the ability of the catalyst to partially oxidize the hydrocarbon to facilitate the NO_x reduction. To investigate the HC oxidation ability, flow reactor experiments were performed over the Ag2, Ag2Pt500, Ag6 and AgPt500 samples, with the equivalent amount of *n*-octane as in the NO_x reduction experiments, however excluding NO.

As NO_2 is a stronger oxidizing agent than oxygen, the ability of the catalyst to oxidize NO to NO_2 was also studied. Hence, the NO oxidation properties of the same samples as above were investigated using the standard experiment parameters, defined above, with 200 ppm of NO but without the reducing agent.

3. Results

This study aims to elucidate the influence of silver loading and low-level platinum doping on the lean NO_x reduction by hydrocarbon SCR. For this purpose, surface characterization (UV–Vis and XPS) as well as oxidation experiments and NO_x reduction activity studies were performed.

3.1. Oxidation state of silver

The specific surface area measurements show high surface area, in the range of 192 + −23 m^2/g (Table 1), for all samples. Further, the oxidation state of the silver species was investigated using UV–Vis and XPS. Previous UV–Vis spectroscopy studies of Ag/Al_2O_3 suggest that ionic silver species (Ag^+) show absorption peaks in the range between 190 and 230 nm [21,22]. Peaks at 290–350 nm are ascribed to partially charged silver clusters of between 2 and 7 atoms in size ($Ag_n^{\delta+}$), while absorption peaks above 390 nm are suggested to derive from metallic silver (Ag^0) [21,22]. The individual absorption spectra, compensated for the contribution from alumina, and the corresponding Gaussian deconvolution peaks are displayed in Fig. 1. The obtained UV–Vis spectrum is, of course, only an average of all absorption processes in the Ag clusters. In addition, various plasmons (Mie and bulk) can be induced in Ag nanoparticles which also can affect the spectra. To account for this, the half-height width of the peaks was closely monitored to ensure that the peaks of the deconvoluted spectra did not deviate from physical underlying phenomena. Furthermore, the deconvolution was carefully performed and the calculations were reprocessed to assure that the possible variations in peak width or peak frequency does not alter the results to a significant degree. The peak at 190 nm is excluded due to the high level of noise. It is observed that the overall UV–Vis absorption increases for the samples in the order Ag2 < Ag2Pt500 < Ag6 < Ag6Pt500. The peaks around 230 and 360 nm are clearly visible for all samples and the peak at 300 nm is visible for the 2 wt% Ag samples. The deconvolution was performed using five peaks as P1 = 230 nm (Ag^+ [21]), P2 = 300 nm ($Ag_n^{\delta+}$ [21]), P3 = 360 nm ($Ag_n^{\delta+}$ [21]), P4 = 425 nm(Ag^0) and P5 = 545 nm (Ag^0). The P4 and P5 peaks were determined by best correlation with the condition of being at wave lengths above 390 nm. The relation between the Ag^+, $Ag_n^{\delta+}$ and Ag^0 in the analyzed samples was determined from the deconvoluted peak area as the sum of the area of the peaks assigned to the specific species divided by the total sum of the peak areas. Due to the accuracy of the peak assignment, the conclusions from the deconvoluted UV–Vis data should only be used as guide lines for arguments and not as a basis for conclusions on its own. The results are summarized in Table 1.

The UV–Vis data indicate that the relation between ionic silver species, small silver clusters and metallic silver particles is similar for the Ag2, AgPt500, Ag6 and Ag6Pt500 samples (Table 1). Furthermore, no additional absorption peaks can be observed for the Pt doped samples. However, at these low platinum concentrations, absorption peaks for Pt can hardly be detected. The overall UV–Vis results indicate that no significant difference can be seen between the four samples, in terms of silver particle constitution.

In addition to the UV–Vis spectroscopy, the samples were investigated using X-ray photoelectron spectroscopy. The binding energy for the $Ag3d_{5/2}$ peak maximum and the distance between the $Ag3d_{5/2}$ and the $Ag3d_{3/2}$ peak maxima were investigated for the Ag2, Ag2Pt500, Ag6 and Ag6Pt500 samples. The results show, for all samples, that the $Ag3d_{5/2}$ peak is centralized around 367.7 eV, similar to the results by Bukhtiyarov et al. [23]. This validates the existence of Ag^+ species, with a peak to peak distance between 5.9 and 6.0 eV, in accordance with literature data [24]. The region where the $Pt4d_{5/2}$ peak should arise was also investigated, although no peak was detected, likely due to the very low content of platinum. The results indicate that the oxidation state of silver does not change with silver loading and/or Pt doping.

3.2. Catalytic performance

3.2.1. Catalytic activity for NO_x reduction

The activity for NO_x reduction under lean conditions was investigated for all samples by flow reactor experiments (Fig. 2). The CO formation (not shown) is less than 35 ppm and similar for all samples at temperatures below 350 °C. Above this temperature the CO formation increases to around 260 ppm (400 °C) for the Ag2, Ag2Pt100, Ag2Pt500 and Ag6 samples. The Ag6Pt100 sample does however show lower CO formation above 350 °C, and for the Ag6Pt500 sample the CO concentration remains below 35 ppm for the entire temperature range studied. With these exceptions, the HC conversion is directly related to the CO_2 formation.

The NO_x reduction for the samples without Pt doping follow a typical volcano shape, with the activity increasing with temperature up to around 350 °C, after which the competing combustion reaction becomes dominant and the NO_x reduction decreases. This is observed as the hydrocarbon conversion increases while the NO_x reduction decreases (cf. top and bottom panels, Fig. 2). The Ag6 sample shows slightly lower NO_x reduction below 325 °C, compared with the Ag2 sample, but displays the highest NO_x reduction above 350 °C, reaching 68%.

Introducing Pt to the samples considerably influences the NO_x reduction. Although the activity for NO_x reduction over the Ag2Pt100 sample resembles that of the corresponding pure Ag/Al_2O_3 sample at low temperatures, it displays a sharp increase above 325 °C with a higher NO_x reduction cf. the Ag2 sample. The Ag2Pt100 sample shows the highest activity for NO_x reduction above 350 °C with a maximum of 79% conversion at 375 °C. For the Ag6Pt100 sample, an increase in the low-temperature activity is observed. However, the activity levels out and drop with a minimum at 325 °C, where after the NO_x reduction is partially recovered as the temperature reaches 350 °C. The high-temperature activity does however not reach that of the Ag6 sample. For the Ag2Pt500 sample the NO_x reduction recovers almost to the level of the Ag2 and Ag2Pt100 samples at high temperatures. The increased low-temperature performance is more prominent for the high-doped Ag2Pt500 and Ag6Pt500 samples and so is the decrease in activity with the minimum at 325 °C. However, the NO_x reduction over the Ag6Pt500 sample decreases severely above 275 °C. The results from the Ag2Pt500 sample show the highest activity at low temperatures, below 325 °C, with a maximum NO_x reduction of 51%

Table 1
Sample denotation, specific surface area (BET) and relation between the areas of the peaks corresponding to Ag^+, $Ag_n^{\delta+}$ and Ag^0 (UV–Vis) of the Ag/Al_2O_3 samples.

Sample composition	Sample name	SSA[a] (m^2/g)	Ag^+[b] (%)	$Ag_n^{\delta+}$[c] (%)	Ag^0[d] (%)
2 wt% Ag/Al_2O_3	Ag2	189	11	38	51
2 wt% Ag/Al_2O_3 w. 100 ppm Pt	Ag2Pt100	176	–	–	–
2 wt% Ag/Al_2O_3 w. 500 ppm Pt	Ag2Pt500	215	14	39	47
6 wt% Ag/Al_2O_3	Ag6	167	17	37	46
6 wt% Ag/Al_2O_3 w. 100 ppm Pt	Ag6Pt100	170	–	–	–
6 wt% Ag/Al_2O_3 w. 500 ppm Pt	Ag6Pt500	182	17	37	46

[a] BET surface area.
[b] Ag^+ ionic silver, P1 = 230 nm [21].
[c] $Ag_n^{\delta+}$ silver clusters P2 = 300 nm and P3 = 360 nm [21].
[d] Ag^0 metallic silver P4 = 415 nm and P5 = 545 nm.

at 300 °C. The decrease in activity, around 325 °C, is observed for all Pt doped samples, regardless of silver loading. The decrease becomes more prominent and starts at lower temperatures as the silver loading is increased and is most pronounced for the Ag6Pt500 sample.

Considering the outlet concentrations of NO and NO_2 during the SCR reaction (Fig. 2, middle panel), the results indicate that the ratio between NO and NO_2 is quite similar for the Ag2 and Ag6 samples, with NO as the dominant NO_x species over the entire temperature range (Fig. 2 middle panel). For the samples doped with 100 ppm Pt (Fig. 2 middle panel), the NO and NO_2 concentration profiles are altered, with a decreasing NO concentration for the Ag2Pt100 sample and an increasing NO concentration for the Ag6Pt100 sample. The NO_2 concentration profile for the Ag2Pt100 sample resembles that for the Ag2 sample, however with slightly higher concentrations of NO_2 at low temperatures. The Ag6Pt100 sample shows a distinct increase in NO_2 at low temperatures, where after the concentration decreases to levels similar to those of the corresponding undoped sample. Over the 500 ppm Pt doped samples, the NO_2 formation is more similar at low temperatures as compared to the 100 ppm Pt doped samples, although the formation of NO_2 is slightly higher over the Ag2Pt500 sample. The two samples show the same NO concentration at 225 °C, where after the two samples display a similar trend, with NO increasing to 325 °C for the Ag6Pt500 sample and a small decrease followed by an increase up to 325 °C for the Ag2Pt500 sample. A small drop in NO concentration can be seen for both samples at 350 °C and thereafter a continued increase. The overall NO concentration is however much higher for the high-loaded Ag6Pt500 sample.

The hydrocarbon conversion during the SCR reaction for the pure and Pt doped samples is shown in Fig. 2, bottom panel. The results show similar trends for all samples, although the low-temperature conversion is higher for the samples doped with 500 ppm Pt. The Ag2Pt100 and Ag6Pt100 samples do however show a significant difference in hydrocarbon conversion, where the low-loaded Ag2Pt100 sample shows lower HC conversion over the entire temperature range, compared to Ag6Pt100. All samples reach approximately the same HC conversion of ~70% at 400 °C.

3.2.2. Oxidative properties

The activity for hydrocarbon oxidation over the Ag2, Ag6, Ag2Pt500 and Ag6Pt500 samples was investigated by flow reactor experiments (Fig. 3). The results show a clear difference in the activation temperature and conversion profile between the pure and the Pt doped Ag–alumina samples. For the Ag2Pt500 sample, the oxidation starts at 250 °C, reaching a maximum HC conversion

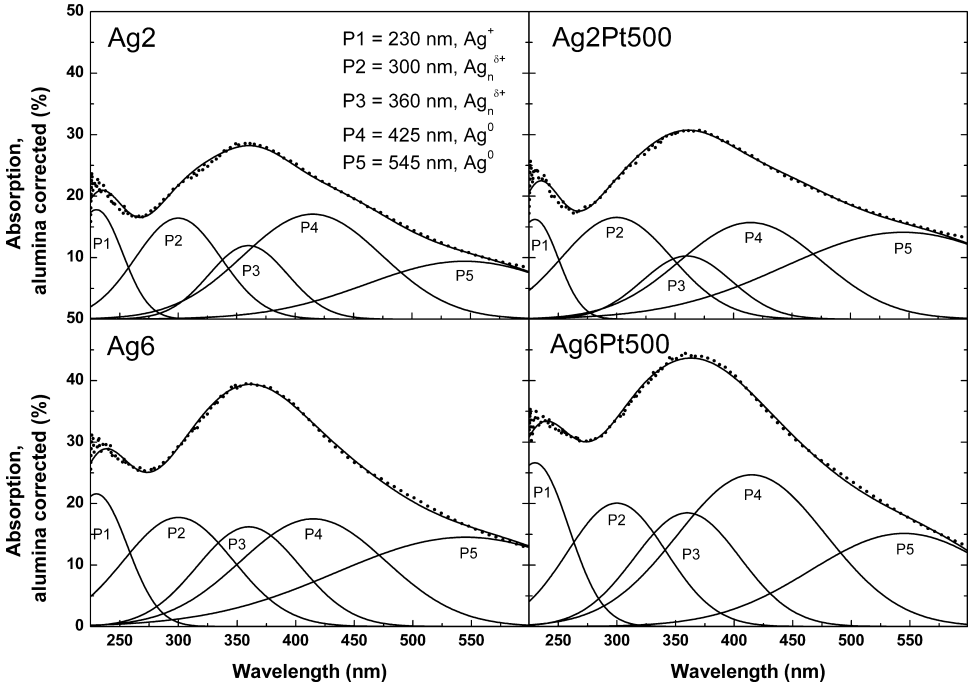

Fig. 1. Absorption spectra (dotted line) with deconvolution peaks for the Ag2, Ag2Pt500, Ag6 and Ag6Pt500 samples. The top solid line shows the sum of the deconvolution peaks.

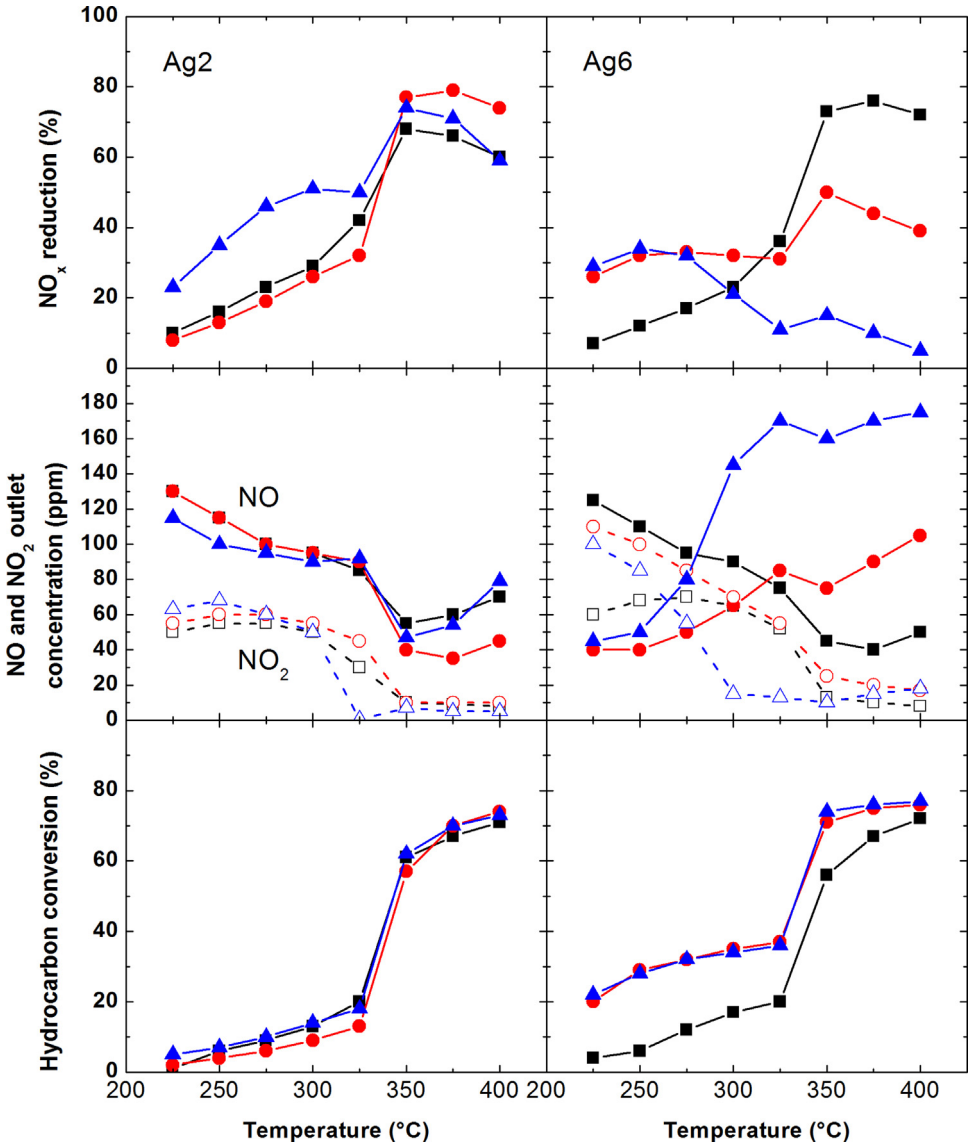

Fig. 2. Flow reactor results for 2 wt% (left column) and 6 wt% (right column) Ag/Al_2O_3 samples without Pt (squares), with 100 ppm Pt (circles) and with 500 ppm Pt (triangles). NO_x reduction (top panel), NO (solid lines, closed markers) and NO_2 (dashed lines, open markers) concentration (middle panel) and hydrocarbon conversion (bottom panel). Inlet gas composition: 200 ppm NO, 10% O_2, 1000 ppm H_2, 5% H_2O, Ar_{bal} and *n*-octane as reducing agent with a C/N molar ratio of 6. GHSV = 33,200 h^{-1}.

of 78% at 400 °C. The HC conversion over the Ag2 sample starts at 300 °C with a maximum conversion of 33% at 400 °C. Over the Ag6 sample the HC conversion starts at the same temperature as for the Ag2 sample. At 350–375 °C however, the HC conversion over the Ag6 sample is lower than over the corresponding 2 wt% Ag sample, but it then increases sharply above 400 °C. Further, the Ag6Pt500 sample shows a HC conversion of 15% already at 225 °C. It can be observed, over this sample, that there seems to be two temperature regimes in regards to the HC conversion, below and above 325 °C. This is similar to the trend of the NO_x reduction (Fig. 2). For the pure Ag samples, the CO formation is almost identical, and the differences in HC conversion are consequently a result of the difference in CO_2 formation.

As NO_2 is a stronger oxidant cf. O_2, an increased NO_2:NO ratio could alter the formation/consumption of other surface species. Flow reactor experiments were performed to study the NO to NO_2 oxidation over the Ag2, Ag2Pt500, Ag6 and Ag6Pt500 samples (Fig. 4).

It is observed that the Ag2 sample shows higher NO_2 formation as compared to the Ag2Pt500 sample, particularly in the temperature range 300–375 °C. This difference increases up to 350 °C, where after it starts to decrease. The Ag6 sample displays the same trend as the Ag2 sample, but with slightly lower NO_2 formation. The Ag2Pt500 and Ag6Pt500 samples show similar concentration profiles, again with higher NO_2 formation for the sample with higher Ag loading (Ag6Pt500). However, comparing the Ag6 and Ag6Pt500 sample, a significant difference in activity for NO oxidation is observed, with a significantly higher NO_2 formation over the Ag6Pt500 sample at low temperatures, which is lower than over the Ag6 sample only between 325 and 350 °C.

4. Discussion

The HC-SCR reaction over metal oxide catalysts consists of several separate reaction steps and the complete reaction scheme is still under debate. However, these steps can in general terms be viewed as oxidation of NO to NO_2 with the subsequent formation of surface nitrates and nitrites, partial oxidation of the hydrocarbon, and finally the reduction of NO_x by the partially oxidized hydrocarbon species forming nitrogen, water and CO_2 [25]. Hence, in a

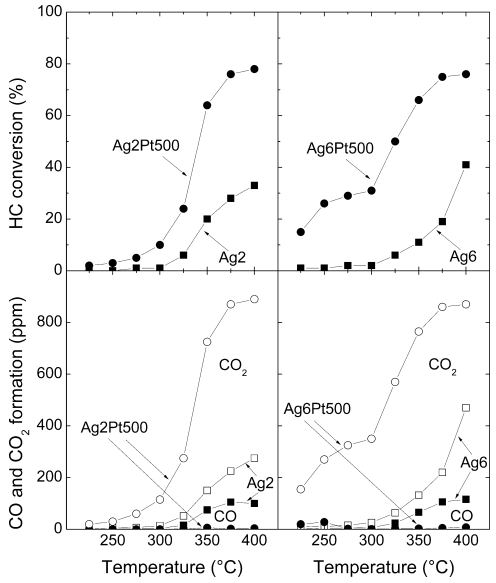

Fig. 3. HC oxidation for the Ag2, Ag2Pt500, Ag6 and Ag6Pt500 samples. Top panel: HC conversion. Bottom panel: CO and CO_2 formation. Inlet gases: 150 ppm *n*-octane, 1000 ppm H_2, 5% H_2O, 10% O_2 with Ar_{bal}. GHSV = 33,200 h^{-1}.

HC-SCR catalyst, sites for both reduction of NO_x and oxidation for HC is present, generally denoted as reduction and oxidation sites, respectively. However, the reaction over a specific site is not limited to only oxidation or reduction. In addition, the complete picture of the promotional effect of hydrogen is still elusive. As the concentration of hydrogen is kept constant during all deNO_x experiments, we chose not to focus on the hydrogen effect in this study. One reaction which particularly requires consideration, as it hinders the selective reduction of NO_x, is the non-selective combustion reaction, where hydrocarbons are completely oxidized by oxygen to water and CO_2. For the Ag–alumina system it has been shown that different forms of oxidized silver species favor the reduction of NO to N_2 [26,27]. Metallic silver particles are, on the other hand, considered to be more active for oxidation reactions [28–30]. Further, it has been suggested that $Ag_n^{\delta+}$ clusters act as highly active sites for the HC-SCR process [26,27], particularly for the activation of the reducing agent by partial oxidation [27]. A silver-based catalyst active for lean NO_x reduction by hydrocarbons thus contains a range of silver species and the balance between small, oxidized Ag species and larger metallic Ag particles is crucial [14,15].

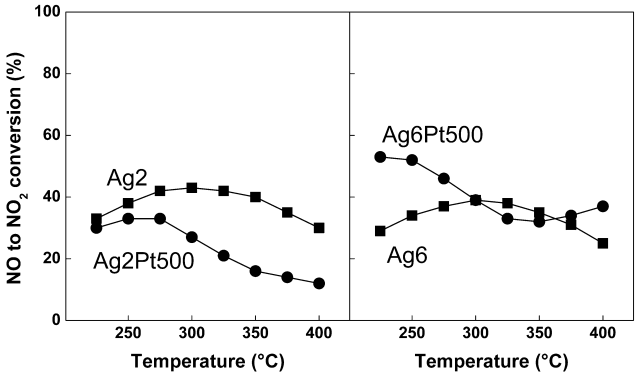

Fig. 4. The NO to NO_2 conversion after NO oxidation in excess oxygen is illustrated for 2 wt% Ag/Al_2O_3 and 2 wt% Ag/Al_2O_3 with 500 ppm platinum (left panel) and for 6 wt% Ag/Al_2O_3 to 6 wt% Ag/Al_2O_3 with 500 ppm platinum (right panel). Inlet gases: 200 ppm NO, 10% O_2, 1000 ppm H_2, 5% H_2O, Ar_{bal}. GHSV = 33,200 h^{-1}.

Table 2
Binding energy for the $Ag3d_{5/2}$ peak maximum and the peak distance between the $Ag3d_{5/2}$ and $Ag3d_{3/2}$ peak maxima for the Ag2, Ag2Pt500, Ag6 and Ag6Pt500 samples. The peak position were shifted with respect to the C1s peak at 284.5 eV to account for charging of the samples [20].

	Ag2	Ag2Pt500	Ag6	Ag6Pt500
BE for $Ag3d_{5/2}$ (eV)	367.6	367.7	367.7	367.7
$Ag3d_{5/2}$– $Ag3d_{3/2}$ (eV)	5.9	5.9	6.0	5.9

In the present study the effect of varying the silver loading of Ag/Al_2O_3 catalysts, as well as the effect of trace amount Pt doping, have been investigated for lean NO_x reduction by *n*-octane. The alumina-based catalysts were synthesized via a sol–gel based method, including freeze drying, which results in a high proportion of non-metallic silver species [14] and exhibit a strong tolerance towards hydrothermal ageing [31]. In addition to NO_x reduction experiments, separate NO and hydrocarbon oxidation experiments were performed. Furthermore, UV–Vis spectroscopy and XPS were used to characterize the silver species of the catalysts. The UV–Vis study reveals the existence of small silver clusters as well as ionic silver species (Table 1), which also have been seen in previous studies on similar samples [16]. In addition, the existence of these sites is also supported by XPS and TEM [15]. Together with the XPS results, the UV–Vis results also indicate that the relation between the integrated areas of the deconvolution peaks for the various silver species is almost constant for all samples, regardless of silver content and Pt doping (Table 2).

The activity for NO_x reduction (Fig. 2, top panels) is relatively low at temperatures below 350 °C for the pure Ag samples. Above 350 °C the NO_x reduction profile differs for the samples, with the highest, high-temperature NO_x reduction reached for the 6 wt% Ag sample. Further, the NO_x reduction results for the Pt doped samples display a relatively high activity at low temperatures but also a dual NO_x reduction activity region, with a local minimum at 325 °C. The dual region phenomenon is least prominent for the Ag2Pt100 sample, where the drop in activity is only visible as a more steep activity increase above 325 °C, while the Ag6Pt100 sample displays a clear dip in activity. As the dopant level is increased, A2Pt500 and Ag6Pt500, the activity drop becomes more pronounced and appears at lower temperatures. The largest decrease in NO_x reduction is observed over the Ag6Pt500 sample, starting already at 250 °C. The Ag6Pt100 sample recovers partly after the activity drop, however the maximum activity is lower as compared to the pure Ag sample. For the Ag6Pt500 sample the second activity maximum at 350 °C is lower than the maximum at 250 °C. Previous studies by Liu et al. [17] show similar behavior when reducing NO over Pt-ZSM-5 catalysts using propene. The authors ascribe the peak in conversion below 300 °C to a higher amount of available hydrocarbon surface species, owing to a change in acidity caused by chlorine from the synthesis, which promotes the adsorption of the hydrocarbons [17]. Further, the second activity peak at higher temperatures is suggested to be owing to the direct NO to N_2 conversion over Pt sites by carbonaceous species. As the platinum precursor in the present study is $Pt(NO_3)_2$ and no other sources of chlorine are present, it is highly unlikely that the presence of Cl should be the cause for the NO_x reduction peak below 300 °C in this work. Furthermore, this effect is not observed for the pure Ag samples. Hence, this effect is likely related to the platinum itself.

Regarding the HC-SCR reaction, Burch et al. [32] and Arve et al. [33] have proposed that the initial step in hydrocarbon activation for further reaction steps, is the abstraction of the first hydrogen from the reductant. The dissociation is related to the sticking probability which is proportionally dependent on the sticking coefficient and exponentially dependent on the dissociative chemisorption energy of the molecule on the surface [34].

Comparing the dissociation energies for different molecules on silver and platinum surfaces, the dissociation energy is always lower for platinum according to Bligaard et al. [35]. The authors report that the dissociative chemisorption for CH_4 on platinum cf. silver differs by 6.49 eV [35], which is a substantial difference. Although the difference likely is smaller for higher hydrocarbons, the sticking probability on platinum is still prone to be higher than on silver. Further, the Brønsted–Evans–Polanyi (BEP) relation [36,37] states that the change in activation energy follows the change in energy of the final state for the chemically dissociated molecule. The metals in the present samples are more or less oxidized, according to the UV–Vis and XPS results. The BEP relation has recently been verified also for oxides [34], which ensures that the activation barrier will be lower for the oxidized Pt particles as well, in relation to the oxidized Ag species. The relative sticking probability should thus be higher over the Pt species than for the corresponding Ag species in our samples.

When comparing the hydrocarbon oxidation results for the 500 ppm Pt doped and pure Ag catalysts (Fig. 3) it can be seen that the HC conversion for the Pt doped samples start at much lower temperatures. For instance, the HC conversion for the Ag2Pt500 sample starts already at 250 °C, which should be compared to well above 300 °C for the corresponding undoped Ag sample. The HC conversion for the Ag6Pt500 sample starts below 225 °C, however the HC conversion drops at 325 °C, similar to the drop in NO_x conversion. Generally, the silver species attain a more metallic state as the temperature increases (>300 °C) [38], which leads to an increase in the rate of HC oxidation, similar to or higher than the rate of adsorption. Hence, the surface coverage of hydrocarbons decreases and other species, e.g. NO_x, can adsorb and react through the HC-SCR path. Moreover, the UV–Vis and XPS results indicate that increasing the silver loading leads to higher total number of silver sites, as the relation between the absorption peak areas for the different Ag species is virtually constant. This is also supported by the results by Kannisto et al. [15]. For the high-loaded Ag samples, this results in an increase in HC oxidation at elevated temperatures. The observed effect is however not entirely clear in the NO_x reduction experiments (Fig. 2), likely due to the influence of NO on the hydrocarbon oxidation, discussed further below. The increased hydrocarbon oxidation over the Pt doped samples at low temperatures, observed in the experiments without NO (Fig. 3) may on the other hand likely derive from an increased adsorption of the hydrocarbon onto the catalytic surface. Furthermore, assuming that incorporation of platinum increases the adsorption of hydrocarbons, the Ag2Pt500 sample should be more susceptible to hydrocarbon poisoning compared to the Ag6Pt500 sample, due to its lower number of oxidation sites. The Ag6Pt500 sample will instead reach similar adsorption/oxidation rates at lower temperatures and hence the overall HC conversion will be higher, also at lower temperatures (<225 °C). Previous studies [14,15,19,39–41] have suggested that the activity for NO_x reduction over Ag–alumina catalysts is affected by several parameters, such as the ratio between oxidation and reduction sites [14,15], the dissociative chemisorption of hydrocarbons [39,40] and, in relation to this, the influence of the C—C bond strength, steric effects and sticking probability, i.e. hydrocarbon-surface interaction [15,41]. The effect of the platinum addition to the silver–alumina system, i.e. higher low-temperature NO_x reduction and a local minimum in activity around 325 °C, could in principle be ascribed to all of these parameters. However, our results also point towards the lower dissociative chemisorption energy for platinum, compared to silver. If so, the platinum may increase the amount of chemisorbed hydrocarbon on the surface and thereby change the required ratio of red/ox sites for efficient partial oxidation of the hydrocarbon. It may also alter the effective oxidation properties of the surface.

Comparing the hydrocarbon conversions over the Ag2 and Ag6 samples in Fig. 2 and 3, a higher HC conversion can be seen in the NO_x reduction experiments (Fig. 2). The conversion for the Ag2Pt500 and Ag6Pt500 samples differs less, however the low-temperature HC conversion is higher for the NO_x reduction experiments cf. the pure Ag samples. The higher HC conversion at low temperatures is likely owing to the presence of reactive nitrite species [42]. As the HC conversion is calculated from the CO and CO_2 formation (Eqs. (3) and (4)), the difference in HC conversion could also be ascribed to the formation of other partially oxidized carbon containing species during the HC oxidation experiments, such as e.g. acetates.

Although platinum is known to be a powerful oxidation catalyst, the NO oxidation experiments reveal that the Ag2Pt500 sample produces lower amounts of NO_2 as compared to the corresponding Ag sample, whereas the Ag6Pt500 sample showed the opposite trend with a higher NO_2 production as compared to the undoped Ag6 sample (except between 300 °C and 350 °C). Previous studies [43] have shown that the inlet NO/NO_2–ratio generally has a negligible influence on the overall NO_x reduction, and that the effect of introducing NO_2 in the feed even is negative for the overall reduction of NO_x when using *n*-octane as reducing agent [43]. Comparing the NO and NO_2 outlet gas composition from the NO oxidation experiments

As no increase is visible in the NO_2 concentration for the doped samples at 325 °C, the drop in NO_x reduction activity can be seen to mainly be a result of a high NO output, possibly due to hydrocarbons blocking the surface. As the NO to NO_2 ratio from the activity study is much more similar compared to that from the NO oxidation experiments it can be assumed that the presence of hydrocarbons strongly affects the NO oxidation behavior.

The overall results show that, as the catalysts are doped with platinum, the oxidation of NO to NO_2 is changed, but as stated before this is not thought to play a major role in the NO_x reduction reaction under the present reaction conditions. No clear trend from the NO oxidation experiments or the NO/NO_2 concentration during the NO_x reduction experiments is found which can explain the change in NO_x reduction activity observed for the platinum doped samples. However, the HC oxidation experiments show that the addition of platinum alters the HC oxidation properties for the Ag–alumina catalysts, resulting in two oxidation regimes (Fig. 3). This behavior, with a local minimum of the HC conversion at 325 °C, is related to the activity for NO_x reduction (Fig. 2) also showing two conversion regimes. As the temperature increases, the amount of available hydrocarbon species on the surface increases, possibly owing to that inactive nitrates desorb allowing more hydrocarbons to adsorb on the surface to a higher degree [42] and to the increased sticking probability for the HC, resulting from the platinum addition and the BEP-relation as discussed above. For the high-loaded samples with 500 ppm platinum the amount of hydrocarbon species starts to poison the surface and the activity for NO_x reduction decreases. As the temperature reaches 350 °C, the hydrocarbon oxidation rate over the pure silver sites exceeds the rate of HC adsorption and the excess hydrocarbon is purged from the surface, resulting in a recovery of the NO_x reduction above the local minimum around 325 °C. Hence, the change in HC oxidation performance and the increase in the hydrocarbon adsorption on the surface are suggested to be the underlying reason for the two regimes of NO_x reduction. This effect leads us to suggest that, although the NO to NO_2 formation likely is of some importance, it is the increase in sticking probability and partial oxidation of the hydrocarbon, owing to the added platinum, that is the main factor leading to the increase in NO_x reduction at low temperatures for the Pt doped samples. This implies that the doped samples have more available hydrocarbon species on the surface, owing to higher

sticking probability, and the increase in low-temperature NO_x reduction is actually a result of this effect.

5. Conclusions

It can be concluded that as the Ag/Al_2O_3 samples are doped with trace-amounts of platinum, the activity for lean NO_x reduction at low temperatures increases. The catalyst composition with the highest activity for NO_x reduction is found to be a 2 wt% loaded Ag/Al_2O_3 sample doped with 500 ppm platinum. This catalyst displays the highest low-temperature activity, which is most likely owing to an increased amount of partially oxidized hydrocarbons on the surface caused by the presence of platinum with lower barrier for dissociative adsorption of the hydrocarbon, as well as a change in the oxidation potential, also attributed to the Pt doping. A higher hydrocarbon adsorption could mean that a lower amount of reducing agent would be required for Pt doped Ag–alumina catalysts as compared to un-doped ones, which is beneficial with respect to fuel efficiency.

Acknowledgements

This work has been performed as part of the MISTRA (The Foundation for Strategic Environmental Research) funded program E4 (Energy Efficient Reduction of Exhaust Emissions from Vehicles), within the Competence Centre for Catalysis (KCK). KCK is financially supported by Chalmers University of Technology, the Swedish Energy Agency and the member companies: AB Volvo, ECAPS AB, Haldor Topsøe A/S, Scania CV AB and Volvo Car Corporation AB. Financial support from Knut and Alice Wallenberg Foundation, Dnr KAW 2005.0055, and Area of Advance Transport are gratefully acknowledged. Carl Wadell at Chemical Physics, Department of Applied Physics, Chalmers University of Technology, is greatly acknowledged for his assistance with the UV–Vis measurements.

References

[1] C. European Parliament, Regulation (EC) No 715/2007 (2007).
[2] R. Detels, D.P. Tashkin, J.W. Sayre, S.N. Rokaw, F.J. Massey, A.H. Coulson, D.H. Wegman, Am. J. Public Health 81 (1991) 350–359.
[3] D. Price, R. Birnbaum, R. Batiuk, M. McCullough, R. Smith, OSTI ID 549660 (1997) 165.
[4] S.I. Matsumoto, CATTECH 4 (2000) 102–109.
[5] K. Skalska, J.S. Miller, S. Ledakowicz, Sci. Total Environ. 408 (2010) 3976–3989.
[6] K. Arve, J.R.H. Carucci, K. Eränen, A. Aho, D.Y. Murzin, Appl. Catal. B: Environ. 90 (2009) 603–612.
[7] K. Arve, K. Eränen, M. Snåre, F. Klingstedt, D. Murzin, Top. Catal. 42–43 (2007) 399–403.
[8] S. Satokawa, Chem. Lett. 29 (2000) 294.
[9] T. Miyadera, Appl. Catal. B: Environ. 2 (1993) 199–205.
[10] R. Burch, J.P. Breen, C.J. Hill, B. Krutzsch, B. Konrad, E. Jobson, L. Cider, K. Eranen, F. Klingstedt, L.E. Lindfors, Top. Catal. 30-31 (2004) 19–25.
[11] H. Kannisto, X. Karatzas, J. Edvardsson, L.J. Pettersson, H.H. Ingelsten, Appl. Catal. B: Environ. 104 (2011) 74–83.
[12] Y. Itoh, M. Ueda, H. Shinjoh, M. Sugiura, M. Arakawa, J. Chem. Technol. Biotechnol. 81 (2006) 544–552.
[13] C.K. Narula, C.S. Daw, J.W. Hoard, T. Hammer, Int. J. Appl. Ceram. Tech.nol 2 (2005) 452–466.
[14] H. Kannisto, H.H. Ingelsten, M. Skoglundh, J. Mol. Catal. A: Chem. 302 (2009) 86–96.
[15] H. Kannisto, K. Arve, T. Pingel, A. Hellman, H. Harelind, K. Eranen, E. Olsson, M. Skoglundh, D.Y. Murzin, Catal. Sci. Technol. 3 (2013) 644–653.
[16] M. Männikkö, M. Skoglundh, H.H. Ingelsten, Appl. Catal. B: Environ. 119–120 (2012) 256–266.
[17] Z. Liu, K.S. Oh, S. Woo, Catal. Surv. Asia 10 (2006) 8–15.
[18] K. Sato, T. Yoshinari, Y. Kintaichi, M. Haneda, H. Hamada, Appl. Catal. B: Environ. 44 (2003) 67–78.
[19] S. Brunauer, P.H. Emmet, E. Teller, J. Am. Chem. Soc. 60 (1938) 309–319.
[20] J.F. Moulder, W.F. Stickle, P.E. Sobol, K.D. Bomben, Handbook of X-ray Photoelectron Spectroscopy, PerkinElmer Corporation - Physical Electronics Division, Eden Prairie, 1992.
[21] N. Bogdanchikova, F.C. Meunier, M. Avalos-Borja, J.P. Breen, A. Pestryakov, Appl. Catal. B: Environ. 36 (2002) 287–297.
[22] A.N. Pestryakov, A.A. Davydov, J. Electron Spectrosc. Relat. Phenom. 74 (1995) 195–199.
[23] V. Bukhtiyarov, V. Kaichev, I. Prosvirin, J. Chem. Phys. 111 (1999) 2169–2175.
[24] A. Manna, B.D. Kulkarni, K. Bandyopadhyay, K. Vijayamohanan, Chem. Mater. 9 (1997) 3032–3036.
[25] R. Burch, Catal. Rev. 46 (2004) 271–333.
[26] J. Shibata, Y. Takada, A. Shichi, S. Satokawa, A. Satsuma, T. Hattori, J. Catal. 222 (2004) 368–376.
[27] K. Shimizu, M. Tsuzuki, K. Kato, S. Yokota, K. Okumura, A. Satsuma, J. Phys. Chem. C 111 (2007) 950–959.
[28] F.C. Meunier, J.P. Breen, V. Zuzaniuk, M. Olsson, J.R.H. Ross, J. Catal. 187 (1999) 493–505.
[29] K.A. Bethke, H.H. Kung, J. Catal. 172 (1997) 93–102.
[30] C. Shi, M.J. Cheng, Z.P. Qu, X.H. Bao, Appl. Catal. B: Environ. 51 (2004) 171–181.
[31] F. Gunnarsson, J.-Y. Zheng, H. Kannisto, C. Cid, A. Lindholm, M. Milh, M. Skoglundh, H. Härelind, Top. Catal. (2013) 1–5.
[32] R. Burch, P. Fornasiero, T. Watling, J. Catal. 176 (1998) 204–214.
[33] K. Arve, F. Klingstedt, K. Eränen, J. Wärnå, L.E. Lindfors, D.Y. Murzin, Chem. Eng. J. 107 (2005) 215–220.
[34] A. Vojvodic, F. Calle-Vallejo, W. Guo, S. Wang, A. Toftelund, F. Studt, J.I. Martinez, J. Shen, I.C. Man, J. Rossmeisl, T. Bligaard, J.K. Norskov, F. Abild-Pedersen, J. Chem. Phys. 134 (2011) 244509.
[35] T. Bligaard, J.K. Nørskov, S. Dahl, J. Matthiesen, C.H. Christensen, J. Sehested, J. Catal. 224 (2004) 206–217.
[36] J.N. Bronsted, Chem. Rev. 5 (1928) 231–338.
[37] M.G. Evans, M. Polanyi, Trans. Faraday Soc. 34 (1938) 11–24.
[38] W.-X. Li, C. Stampfl, M. Scheffler, Phys. Rev. Lett. 90 (2003) 256102.
[39] K. Ruth, R. Burch, R. Kieffer, J. Catal. 175 (1998) 27–39.
[40] K. Arve, F. Klingstedt, K. Eranen, L.E. Lindfors, D.Y. Murzin, Catal. Lett. 105 (2005) 133–138.
[41] H. Härelind, F. Gunnarsson, S.M.S. Vaghefi, M. Skoglundh, P.-A. Carlsson, ACS Catal. 2 (2012) 1615–1623.
[42] K. Shimizu, J. Shibata, H. Yoshida, A. Satsuma, T. Hattori, Appl. Catal. B: Environ. 30 (2001) 151–162.
[43] D. Creaser, H. Kannisto, J. Sjöblom, H.H. Ingelsten, Appl. Catal. B.: Environ. 90 (2009) 18–28.